

SIMULATION STUDY OF A DOGBONE DAMPING RING

Y. Ohnishi* and K. Oide, KEK, Oho, Tsukuba, Ibaraki 305-0801, Japan

Abstract

Damping ring is one of the major issues in the future linear collider (ILC). We discuss the design of the dogbone damping ring and its performance including the emittance growth and the dynamic aperture related to the nonlinearities of the wigglers and the space charge effects. In this paper, we use the ring lattice borrowed from A. Wolski (Version 6.4.1).

INTRODUCTION

A unique characteristic of the dogbone damping ring[1] is its circumference, 17 km, as shown in Table 1. The long circumference is suitable for the pulse structure of the linear collider with a relatively conservative scheme of the injection and the extraction. The dogbone damping ring has a long straight section to reduce the construction efforts by sharing a part of tunnel with the main linac. Therefore, one of the complications is the space charge effects which arise in the long straight beam-line, even though an xy-coupling try to reduce those effects. In addition, a long wiggler section is necessary for the dogbone compared with conventional designs to obtain the enough damping time while keeping the equilibrium emittance small. Another complication comes from nonlinear effects of the wiggler magnets[2]. In this article, we present results of tracking simulations for the wiggler nonlinear effects and the space charge effects in the dogbone damping ring.

Table 1: Machine parameters of the dogbone damping ring.

Parameter	Symbol		Unit
Energy	E	5	GeV
Circumference	C	17	km
Betatron tunes	ν_x/ν_y	76.31/41.27	
Synchrotron tune	ν_s	-0.071	
Emittance	ε_x	5×10^{-6}	m
Bunch length	σ_z	6	mm
Momentum spread	σ_δ	0.13	%
Momentum compaction factor	α_c	1.24×10^{-4}	
Energy loss per turn	U_0	20.4	MV
RF frequency	f_{RF}	500	MHz
RF voltage	V_c	50	MV
Wiggler bend radius	ρ_w	10	m
Wiggler length	L_w	468	m
Wiggler period	λ_w	0.4	m
Long. damping time	τ_d	28	msec
Particles/bunch	N	2×10^{10}	
Chromaticities	ξ_x/ξ_y	-124/-56	

* yukiyoshi.onishi@kek.jp

WIGGLER FRINGE FIELD

The total Hamiltonian in the vertical plane of the ring into which wigglers are inserted can be expressed by[3]

$$H = H_0 + \frac{L_w}{4\rho_w^2} y^2 + \frac{L_w}{12\rho_w^2} k^2 y^4, \quad (1)$$

where H_0 is the Hamiltonian without the wigglers, L_w is the length of the wiggler section, ρ_w is the bending radius of the wiggler, $k = 2\pi/\lambda_w$, λ_w is the period length of the wiggler. Therefore, the associated betatron tune shift due to the wigglers is obtained from

$$\Delta\nu_y = \frac{\bar{\beta}_y}{4\pi} \left(\frac{L_w}{2\rho_w^2} + \frac{L_w}{3\rho_w^2} k^2 y^2 \right), \quad (2)$$

where $\bar{\beta}_y$ is the averaged vertical beta function in the wiggler section.

Alternatively, the Hamiltonian is parameterized by using an action variable,

$$H = 2\pi \left(\nu_{x0} J_x + \nu_{y0} J_y + \nu_{z0} J_z + c_{xx} J_x^2 + c_{yy} J_y^2 + c_{zz} J_z^2 + c_{xy} J_x J_y + c_{yz} J_y J_z + c_{zx} J_z J_x + \dots \right). \quad (3)$$

In the case of $J_x = J_z = 0$, the vertical betatron tune can be approximately written by

$$\nu_y = \frac{1}{2\pi} \frac{\partial H}{\partial J_y} = \nu_{y0} + 2c_{yy} J_y. \quad (4)$$

By comparing Eq. (2) with Eq. (4), the amplitude dependence of the vertical betatron tune due to the wigglers can be calculated by

$$c_{yy} = \frac{\bar{\beta}_y^2 L_w k^2}{12\pi\rho_w^2}. \quad (5)$$

In order to investigate dynamic apertures of the ring described in the later section, we perform a particle-tracking simulation by using SAD[4]. SAD is a integrated code for optics design, particle tracking, machine tuning, etc., and has been used for years at several machines such as KEKB and KEK-ATF. In SAD, the wiggler bending field is approximated by trapezoids, and the Hamiltonian up to $O(y^4)$ are included in the model. Therefore, the primary nonlinear effect of the fringe field of the wiggler magnets are included in the tracking by SAD. Table 2 shows the nonlinear coefficient, c_{yy} , estimated by the tracking with and without the nonlinearity of the wigglers. The difference between with and without the nonlinearity is +6070 from Table 2. Using Eq. (5), the nonlinear coefficient due to the wigglers can be calculated to be +5920 analytically, using $\bar{\beta}_y = 13.8$ m and the parameters in Table 1. Consequently, the tracking simulation well reproduces the octupole-like component of the wigglers. Table 2 also shows the nonlinear coefficient with and without sextupole magnets. The contribution of the nonlinear effects is about -9000 from the sextupole magnets.

Table 2: Nonlinear coefficient c_{yy} of the damping ring estimated by the tracking simulations.

sextupoles	w/o nonlinear wig.	w nonlinear wig.
ON	-1230	+4840
OFF	+7630	+13780

SPACE CHARGE EFFECT

In this simulation, the space charge is calculated in two steps: (1) calculate the equilibrium 6D beam envelope including the synchrotron radiation and the space charge effect, and (2) track particles with a weak-strong model assuming the beam envelope obtained from (1). We assume $N = 2 \times 10^{10}$ and the minimum coupling $\varepsilon_y/\varepsilon_x = 0.2\%$. The space charge force is applied at the entrance of about 10,000 elements all over the ring, and calculated with a Gaussian distribution in all coordinates. We have applied an ultra-relativistic approximation to obtain the space-charge potential as

$$V(x, y, z) = U(x, y) \frac{1}{\sqrt{2\pi\sigma_z}} \exp\left(-\frac{z^2}{2\sigma_z^2}\right), \quad (6)$$

where $U(x, y)$ is a two-dimensional electrostatic potential for the Gaussian beam distribution. The potential U is basically a function of X/σ_X , Y/σ_Y , and $r = \sigma_Y/\sigma_X$, where X and Y denote the major and minor axes of the beam. We approximate U by cubic splines in these parameters to calculate the force, and it satisfies the symplectic condition up to the machine precision.

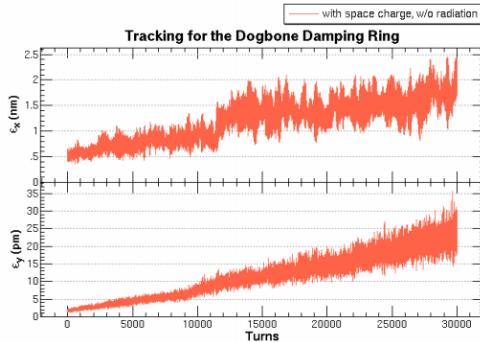


Figure 1: The horizontal(upper) and the vertical(lower) emittance growth due to the space charge effect. The synchrotron radiation is turned off. The emittances increase almost linear in time. It will be safe if the growth rate is much smaller than the synchrotron radiation excitation.

We have tracked particles with this space-charge model of the dogbone damping ring and estimated the emittance growth. Typically, the emittance increases linearly in the number of turns as shown in Fig. 1. It looks like a diffusion process due to the nonlinear component of the force. Thus, we can estimate the diffusion rate for the given lattice tunes, (ν_x, ν_y) . The result is shown in Fig. 2. Although several

resonance lines which cause the emittance growth are seen, there remains wide area in the tune space where the growth rate is less than 20% of the radiation excitation.

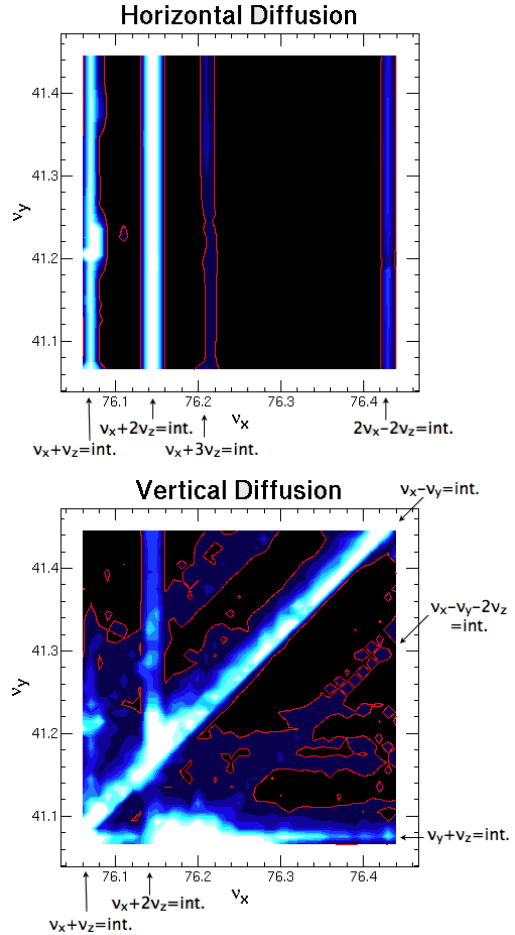


Figure 2: The tune space of the horizontal(upper) and vertical(lower) emittance diffusion rate due to the space charge effect. Darker area has smaller diffusion rate, and the red line shows 1/5 of the synchrotron radiation excitation. Several resonance lines are seen.

DYNAMIC APERTURE

The dynamic aperture can be defined as a stability for one damping time. The damping time of the dogbone ring is 28 msec which corresponds to 500 turns. It is difficult to apply an analytic approach or a perturbation method because the strong sextupole magnets and the long wiggler section cause the strong nonlinearity. Therefore, we estimate the dynamic aperture by the tracking simulation. We perform the tracking by SAD to investigate dynamic apertures. Six canonical variables, $x, p_x, y, p_y, z,$ and δ are used to describe the motion of a particle, where p_x and p_y are transverse canonical momenta which are normalized by the design momentum, p_0 , and δ is the relative momentum deviation from p_0 . We limit the initial conditions to $y = x, p_{x0} = 0, p_{y0} = 0,$ and $z = 0$ to evaluate the acceptance of

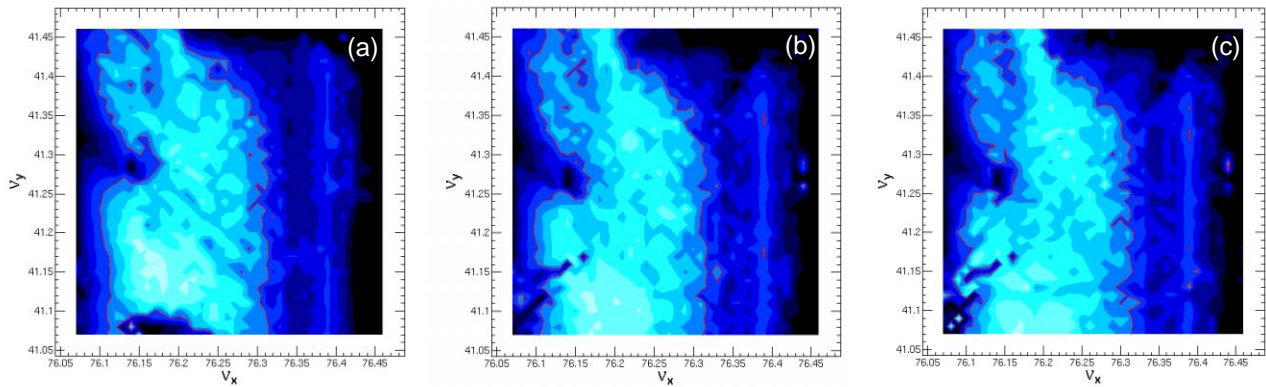


Figure 4: Tune survey of the dynamic aperture: (a) without wiggler nonlinearity and space charge, (b) with wiggler nonlinearity, without space charge, (c) with wiggler nonlinearity and space charge. The red lines show acceptable regions.

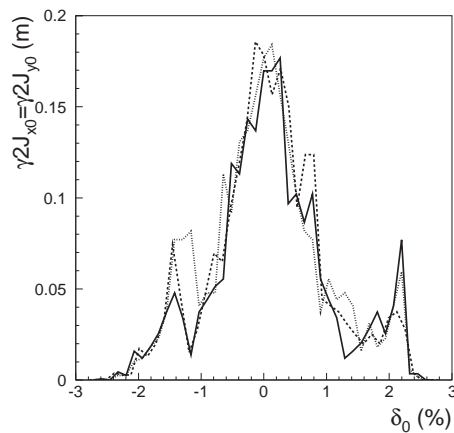


Figure 3: Comparison of the dynamic aperture including the wiggler nonlinearity and the space charge effect (solid), the wiggler nonlinearity without the space charge (dotted), and without both (dashed).

the injected beam rather than the lifetime at the equilibrium state. The injected beam is a round shape in the transverse direction and coherent oscillations due to injection kickers are negligible. We also survey a momentum aperture within $\pm 3\%$. As a criterion of the stability, the maximum amplitude of the particle orbit is within 10 cm in the x and y coordinate during 500 turns of the tracking.

Figure 3 shows the dynamic apertures obtained from the tracking simulations without and with the wiggler nonlinearity and the space charge effect. No machine error is included in the lattice. The transverse acceptance for the initial condition is expressed by $\gamma 2J_{x0} = \gamma 2J_{y0}$, where $2J_{x,y}$ is the Courant-Snyder invariant and γ is the Lorentz factor. Momentum acceptance is expressed by δ_0 which is the initial momentum deviation from the design momentum. The working point is $\nu_x/\nu_y = 76.31/41.27$. There is no significant difference between with and without wiggler nonlinearity and the space charge. Figure 4 shows tune surveys of the dynamic apertures. The initial condition of the

transverse acceptance is also restricted by $\gamma 2J_{x0} = \gamma 2J_{y0}$. The aperture is defined by the minimum acceptance within the momentum range of $\pm 1\%$. The lighter color indicates the larger dynamic aperture and the red contour shows 2σ of the injected beam size. The normalized emittance of the injected beam is assumed to be 0.1 m in the horizontal and vertical plane. The third order resonance is found in the horizontal tune. However, the dynamic apertures can be kept sufficient for the injected beam assumed here even though wiggler nonlinearity and/or the space charge effect are included in the tracking simulations.

CONCLUSION

We have studied the emittance growth due to the space charge and the dynamic apertures with the nonlinear components of the wigglers together with the space charge. Results from the simulations show that those are all within the acceptable level for requirements of the linear collider. There are big area in the tune space where those effects are not serious. Further study with orbit and optical errors should be carried out to realize the project.

The authors thank A. Wolski for providing us the MAD deck of the dogbone lattice, H. Koiso for converting MAD deck to SAD, K. Kubo and M. Kuriki for giving opportunities to join the study in the ILC Working Group.

REFERENCES

- [1] "TESLA Technical Design Report", TESLA Report 2001-23, DESY 2001-011, March, 2001.
- [2] D. Sagan *et al.*, "A Magnetic Field Model for Wigglers and Undulators", ICFA Beam Dyn. Newslett. 31:48-52, 2003
- [3] J. Gao, "Analytical Estimation of Dynamic Apertures Limited by the Wigglers in Storage Rings", Proceedings of PAC03, p. 3267.
- [4] K. Oide, Nucl. Inst. Meth. A 276, 427 (1989). <http://acc-physics.kek.jp/SAD/sad.html>.